HEAT TRANSFER AND FLUID FLOW IN STATIONARY GTA WELDING OF γ-TiAl BASED ALLOYS: EFFECT OF THERMOCAPILLARY FLOW

N. El-Kaddah, M. Arenas and V. L. Acoff

Department of Metallurgical and Materials Engineering
The University of Alabama
Tuscaloosa, AL 35487-0202 USA

ABSTRACT

Numerous welding and joining studies dealing with the weldability and weld properties of gamma based titanium aluminide (γ-TiAl) alloys have been performed to date. However, there have been no reported studies in the open literature on the theoretical predictions of the weld pool geometry of γ-TiAl. In this paper, model predictions and experimental data were used to determine the effect of surface tension driven flow on the shape of welds in γ-TiAl alloys. Stationary welds were produced in Ti-48Al-2Cr-2Nb (atomic %) using autogenous gas tungsten arc (GTA) welding at an arc current of 75 A for 1.0 second. The weld pool depth and width were measured from the actual weldments and the theoretical predictions were determined from the mathematical model developed from the solution of the electromagnetic field, fluid flow and heat transfer equations. The surface tension-temperature coefficient of molten γ-TiAl was estimated from comparison of the model predictions to the experimental data and it was found that the best agreement between the two occurred for the reference case of zero surface tension forces. The results of this study suggest that the surface tension of γ-TiAl alloys is almost independent of temperature.

NOMENCLATURE

B   magnetic flux density
C_p specific heat
f   liquid fraction
g   gravity
F   electromagnetic force
I   current
J   current density
k   thermal conductivity
L   latent heat of melting
P   pressure
q   heat flux
R_c effective arc radius
R_s effective radius of heat distribution
t   time
T   temperature
U   velocity
σ   electrical conductivity
μ   magnetic permeability
ρ   density
τ   viscous shear stress tensor
β   thermal expansion coefficient
γ   surface tension
η   arc efficiency

INTRODUCTION

Gas tungsten arc (GTA) welding is the principal welding technique for joining and manufacturing gamma titanium aluminide (γ-TiAl) components for turbine and automobile engines (Kelly, 1992). Despite the extensive use of this welding technique for these alloys to date, the scientific basis of the GTA operation has been concerned with the structural characterization of the final weld rather than the physics of the arc welding process. There is much to be understood about the way changes in various operating parameters affect weld geometry, weld penetration and mechanical properties of the final weld.

Figure 1 shows a sketch of a typical GTA system where it is shown that an arc is stuck between the tungsten electrode and the metal. The thermal energy generated in the arc, which depends on the arc current, melts the local area to form a pool. The passage of the arc current through the base metal also dissipates its energy as heat (Joule heating) and gives rise to an electromagnetic force field. This force field produces recirculating motion opposite to the natural convection currents. The presence of high temperature gradients at the free surface will also induce thermocapillary flow from low to high surface tension regions, only if the surface tension of the molten metal is temperature dependent. The superposition of the electromagnetic, buoyancy and surface tension driven flows results in a complex flow pattern with spatially variable heat transfer rates, which will not only affect the transient evolution of the temperature profiles, but also the development of the weld pool geometry.
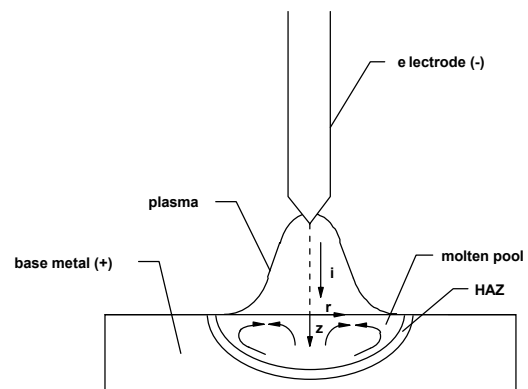
Figure 1. Schematic of the gas tungsten arc welding pool.

In recent years, considerable progress has been made regarding our understanding of fluid flow and heat transfer phenomena in GTA welding processes through mathematical modeling. Kou and Sun (1985), Kim et al. (1997) and Szekely and co-workers (1984, 1989) have investigated the role of buoyancy, surface tension and electrically driven flows on the development of the weld pool. It has been shown that counterclockwise melt circulation characteristic of electromagnetically driven flow promotes weld penetration, while the clockwise recirculating flow of natural and thermocapillary flows produces shallow welds. It has also been shown that weld penetration strongly depends on the surface tension-temperature coefficient, which is a material property.

While the modeling approach has provided insight into the role of fluid flow and heat transfer in GTA welding, the application of the models to simulate actual γ-TiAl welding operation requires more information than is available at present. Specifically, information such as the heat and current flux distributions on the surface in terms of key welding parameters, namely arc current and voltage, arc gap and electrode tip angle, are required. In addition, there is no published data in the open literature on the surface tension-temperature coefficient of γ-TiAl alloys.

The purpose of this work is to generate such information experimentally and to formulate a corresponding model to accurately predict the weld pool geometry. The present paper is concerned with experimental measurement of welding arc characteristics and the estimation of surface tension-temperature coefficient of γ-TiAl through direct comparison between the model predictions and the experimental data.

MODEL FORMULATION

The mathematical description of arc welding involves the solution of the electromagnetic field, the fluid flow and heat transfer equations, together with constitutive equations describing heat transfer and current flow from the arc to the metal. For the system shown in Figure 1, the arc is characterized by axial symmetry thus, rendering the problem to be two-dimensional in the r and z cylindrical coordinate system. The problem is solved by the following equations.

Electromagnetic Field

The current density distribution in the metal, $J(J_r,0,J_z)$, was calculated by solving the magnetic diffusion equation for the azimuthal magnetic field, $B(0, B_\theta,0)$, which for a static field may be written as:

$$\left[\nabla . \hat{\sigma} \nabla B\right]_{\hat{e}} = 0 \qquad (1)$$

where σ is electrical conductivity of the metal.

The boundary condition for B along the top surface of the base metal is obtained from the current density J in the arc-striking region. In this model, the current distribution is represented by the following Gaussian distribution function from Tsai and Eagar (1985):

$$J_z\big|_r = \frac{3 I}{\pi R_c^2} \exp\left(-\frac{3 r^2}{R_c^2}\right) \qquad (2)$$

where I is arc current and R_c is the arc radius at the surface of the metal, which is a measurable quantity.

From this equation and using Ampere's law, B at the top metal surface is

$$B_\theta\big|_r = \frac{3 \mu I}{\pi r R_c^2} \int_0^r \exp\left(-\frac{3\zeta^2}{R_c^2}\right)\zeta \, d\zeta \quad at \ z = 0 \quad (3)$$

where μ is magnetic permeability. From the solution of the magnetic field, the current density can be readily computed from Ampere's law ($\nabla \times B = \mu J$), which is then used to compute the electromagnetic force, $F_{em}(F_r,0,F_z)$:

$$F_{em} = J \times B \qquad \textbf{(4)}$$

Heat Transfer

The governing equation describing conductive, convective and phase change processes in the solid, liquid and mushy regions of the metal was represented by the following differential equation:

$$\rho C_p\left[\frac{\partial T}{\partial t} + (U \cdot \nabla)T\right] = \nabla . k\nabla T + \frac{J^2}{\sigma} - L\frac{df}{dt} \quad (5)$$

where t is time, T is temperature, U is velocity, ρ is density, C_p is specific heat, k is thermal conductivity, L is latent heat of solidification and f is liquid fraction in the mushy region.

Assuming that f varies linearly with temperature as,

$$f = \frac{T - T_s}{T_l - T_s} \qquad (6)$$

equation 5 may be expressed as

$$\rho C_p^*\left[\frac{\partial T}{\partial t} + (U \cdot \nabla)T\right] = \nabla . k\nabla T + \frac{J^2}{\sigma} \qquad (7)$$

where

$$C_p^* = \begin{cases} C_{p,s} & T \leq T_s \\ C_{p,s} + \dfrac{L}{T_l - T} & T_s \leq T \leq T_l \\ C_{p,l} & T \geq T_l \end{cases}$$

C_p^* is a modified specific heat, and T_s and T_l are the solidus and liquidus temperatures, respectively.

The thermal boundary condition at the top surface is

$$-k\left(\vec{n} \cdot \nabla T\right) = q_s - q_c - q_r \qquad (8)$$

where q_s is the heat flux from the plasma jet to the metal surface, while q_c and q_r are the convective and radiative heat losses, respectively. In this model, the heat flux from the source is represented by:

$$q_s = \frac{3 V I\eta}{\pi R_s^2} \exp\left(-\frac{3 r^2}{R_s^2}\right) \quad at \ z = 0, \quad r \leq R_s \quad (9)$$

where V is arc voltage, η is welding efficiency, and R_s is the effective radius of the power distribution. The heat distribution parameter, R_s, is directly related to the arc

radius R_c, and the dependence between these two parameters was taken from Tsai and Eagar (1985).

Fluid Flow

Since the viscous relaxation time of the flow in the weld pool is much smaller than the time scale of melting, the fluid flow problem may be regarded as time-independent within the time frame of melting. This considerably simplifies the numerical problem since the fluid flow equations have to be solved only when there is a change in the weld pool shape. The flow in the molten pool was also assumed to be laminar. Under the above assumptions, the equations to be solved are as follows:

Conservation of mass:

$$\nabla \cdot (\rho U) = 0 \qquad (10)$$

Navier-Stokes equation:

$$\rho (U \cdot \nabla) U = -\nabla p - \nabla \cdot \tau + \rho g ((1 - \beta (T - T_l)) + F_{em} \quad (11)$$

where τ is viscous shear stress tensor, p is pressure, and β is thermal expansion coefficient.

The boundary conditions for this problem, which account for surface tension driven flow, are zero velocity at solid surfaces, zero shear stress at the symmetry axis, and the balance between the rate of momentum transfer and surface tension forces at the free surfaces, which may be expressed as:

$$\tau_{rz} = \frac{\partial \gamma}{\partial T} \frac{\partial T}{\partial r} \qquad at \quad z = 0 \qquad (12)$$

where γ is the surface tension of the molten metal.

Equations (1) to (12) together with the associated boundary conditions represent the complete mathematical description of the model. These equations, which were cast in cylindrical coordinates, were solved numerically using the control volume technique. In this study, calculations were carried out using a 36 X 36 grid with fine mesh in the melting region and near the free surface.

EXPERIMENTAL PROCEDURE

Autogenous GTA welds were produced on 15 x 15 x 2 (mm) coupons of Ti-48Al-2Cr-2Nb (atomic %) coupons using spot welding (i.e. welding with the torch stationary at a single location for a fixed time). The coupons were placed on top of a thick titanium aluminide block and their surfaces were polished in order to provide good electrical contact. Welding was performed in a purge chamber back-filled with argon to provide an inert atmosphere and to reduce atmospheric contamination. A 1.02 mm diameter tungsten electrode with a truncated conical tip angle of 20° was used. All samples were spot welded using straight polarity, direct current of 75 A. The arc gap between the tip of the electrode and the metal was 5 mm. All experiments were carried out for a welding time of 1.0 second. The welding operating parameters are summarized in Table I.

The actual measurements taken included the determination of the radius of the arc on the metal surface, which is the only unknown parameter in the model, and the

measurement of the weld pool profile. Measurement of the arc radius was accomplished using conventional photographic techniques. Filming of the arc was carried out using an EPSON digital camera with automatic electronic shutter time ranging from 1/30 to 1/10,000 s. A number 9 welding filter was used to obtain sharp images for accurate determination of the arc radius. The welded specimens were cut into sections and prepared for light microscopy analysis using conventional metallographic techniques. The etchant used was Kroll's modified reagent which consisted of 100 ml H_2O + 35 ml H_2O_2 + 5 ml HNO_3+ 10 ml HF. The light micrographs of the weld zone, taken at a magnification of 50X, were used to determine the quantitative measurement of the weld pool depth, width and geometry.

Welding parameter	Value
Welding current	75 A
Arc voltage	16 V
Arc gap	5 mm
Current distribution parameter R_c	4.25 mm
Electrode tip angle	20 deg
Power input	1200 W
Argon flow rate	10 L/min
Electrode diameter	1.02 mm
Arc efficiency	43 %

Table I. Arc parameter data

RESULTS AND DISCUSSION

In the following, we shall present a selection of both the experimental measurements and theoretical predictions for the welding conditions given in Table I. The calculations were performed using the physical and thermal properties of γ-TiAl shown in Table II. All property values, except for surface tension, used in the calculations were taken from Li et al. (1996). In the absence of reliable surface tension data for γ-TiAl, computed results were generated over a range of surface tension-temperature coefficients characteristic of molten metal, ranging from 0 to -0.0002 N $(m.K)^{-1}$ (Pelzel, 1950 and Allen, 1963).

To apply the model to predict the weld pool geometry of γ-TiAl welds, the effective current distribution parameter, R_c, must be first determined. Figure 2 shows a typical photograph of the welding arc. This photograph clearly shows the hot ionized gas between the tungsten electrode and the base metal. Since the electric discharge is confined to the hot plasma, the effective radius of the current distribution parameter is essentially that of the plasma jet at the surface of the base metal. Under the welding conditions employed, R_c was estimated to be 4.25 mm.

Figure 3 shows the computed electromagnetic force vectors in the base metal. The solid line is the computed weld pool shape after one second for the reference case of zero surface tension. This figure shows that the

electromagnetic force field is predominately in the radial direction and pointing toward the axis of symmetry. Also, it shows that the force field decays rapidly below the top surface. The force at the free surface exhibits a maximum at about 2 mm from the axis of symmetry, which is approximately one half the radius of the arc at the metal surface. These results not only confirm previous findings that the electromagnetic forces generate counterclockwise recirculating flow, but also suggest that the intensity of melt circulation driven by electromagnetic forces depends on the size of the weld pool. The mean velocity of electromagnetic driven flow is expected to increase with the weld pool radius until it reaches a maximum at one half the arc radius (the case shown in Figure 3). For wider weld pools, due to the attenuation of the electromagnetic force field, surface tension and buoyancy forces are likely to have a stronger influence on the direction and magnitude of melt velocities.
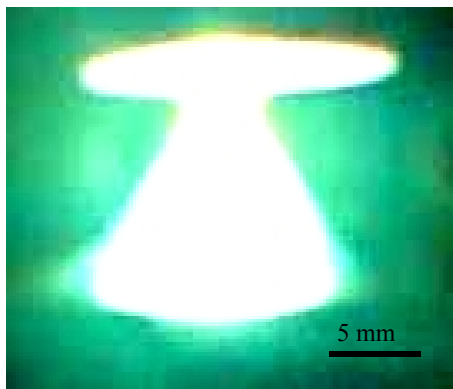
Figure 2: A photograph of the welding arc; I=75 A, Arc gap = 5 mm
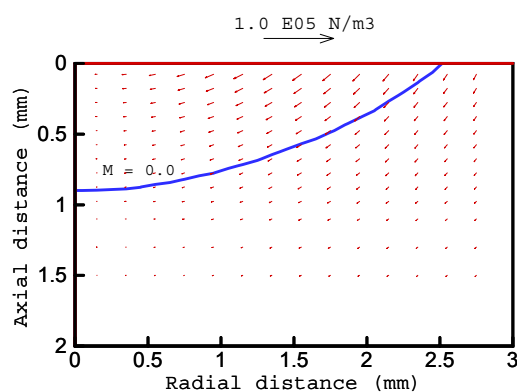
Figure 3: Computed electromagnetic force field.

Physical constants	Value
Density ρ, kg/m^3	3636
Thermal expansion coefficient β_T, °K^{-1}	10^{-4}
Thermal conductivity κ, W/m.°K	11.0
Latent heat of fusion L, J/kg	3.77×10^5
Specific heat C_p, J/kg°K	727
Viscosity μ, kg/m.s	3.6×10^{-3}
Electrical conductivity σ, (ohm.m)$^{-1}$	1×10^6
Solidus temperature, °C	1491
Liquidus temperature, °C	1512

Table 2: Physical constants of TiAl

The effect of thermocapillary flow on temperature and velocity fields is shown in Figures 4 to 6. Figure 4(a) shows the computed temperature profile in the molten pool after 1 s of welding while Figure 4(b) shows the corresponding velocity field in the absence of surface tension driven flow. The velocity field exhibits the characteristic counterclockwise recirculating loop caused by electromagnetic forces with a maximum velocity of 0.02 m/s. The temperature field resulting for this flow shows a significant temperature gradient with a maximum temperature of 2100°C. Figures 5 (a)-(b) and 6 (a)-(b) show the corresponding plots for the cases where allowance has been made for thermocapillary flow. The computed weld pool shape temperature and velocity fields for these cases are drastically different from the computed ones in the absence of surface tension forces. The weld pool is shallower and wider as would be expected. The velocities are an order of magnitude larger and the main recirculating loop has reversed its direction to clockwise rotation. Furthermore, there is also a significant reduction in the weld pool temperatures with the maximum temperature reaching about 1800°C. It is interesting to see that doubling the value of the surface tension-temperature coefficient from -0.0001 and -0.0002 N.(m.K)$^{-1}$ has little effect on the weld pool geometry and temperature profile in the weld pool.

The parametric study presented here has clearly shown the role that thermocapillary flow could play in the development of the weld pool. The key issue now is to resolve the actual effect of surface tension forces in GTA welding of γ-TiAl alloys. Figure 7 shows a comparison between the experimentally observed weld pool shape and the theoretical predictions for the three surface tension-temperature coefficients used in the parametric study. Inspection of this figure shows that the best agreement between measurements and predictions regarding both the depth and the width of the weld pool is for the reference case of zero surface tension forces. This would suggest that the surface tension-temperature coefficient of γ-TiAl is either zero or too small to affect the temperature and velocity fields in the weld pool.
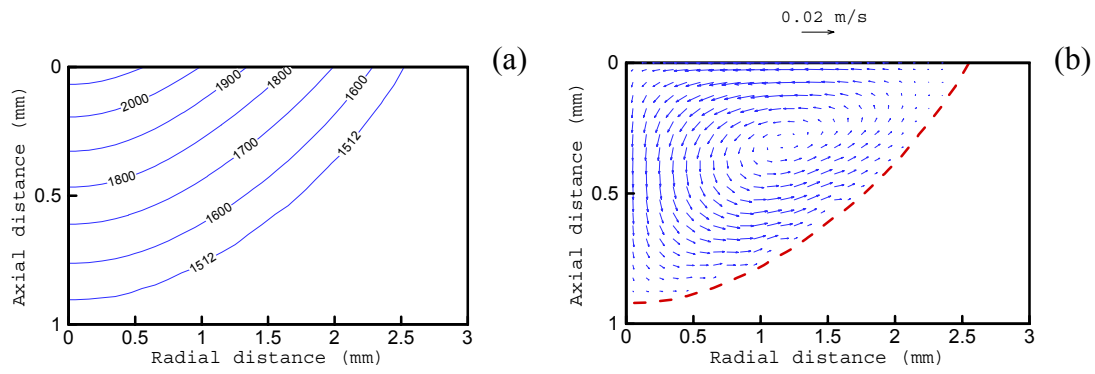
Figure 4. Computed temperature and velocity fields after 1s for $\dfrac{\partial \gamma}{\partial T} = 0$: a) temperature, b) velocity.
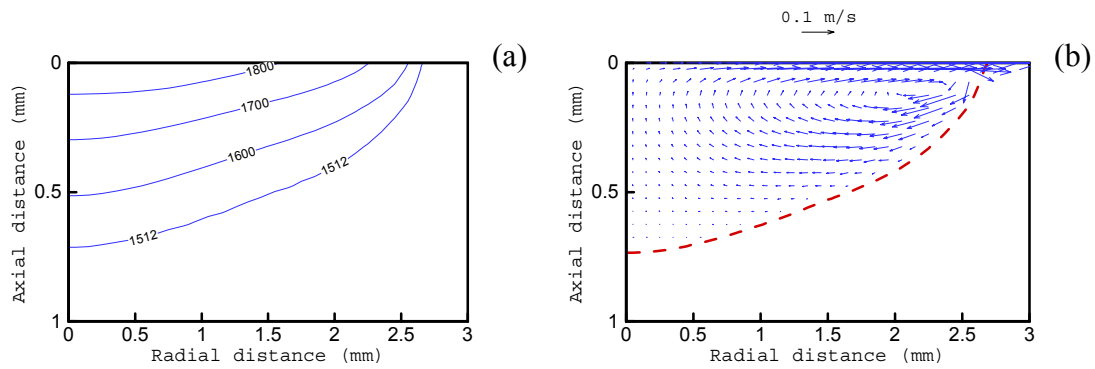
Figure 5. Computed temperature and velocity fields after 1s for $\dfrac{\partial \gamma}{\partial T} = -0.0001$: a) temperature, b) velocity.
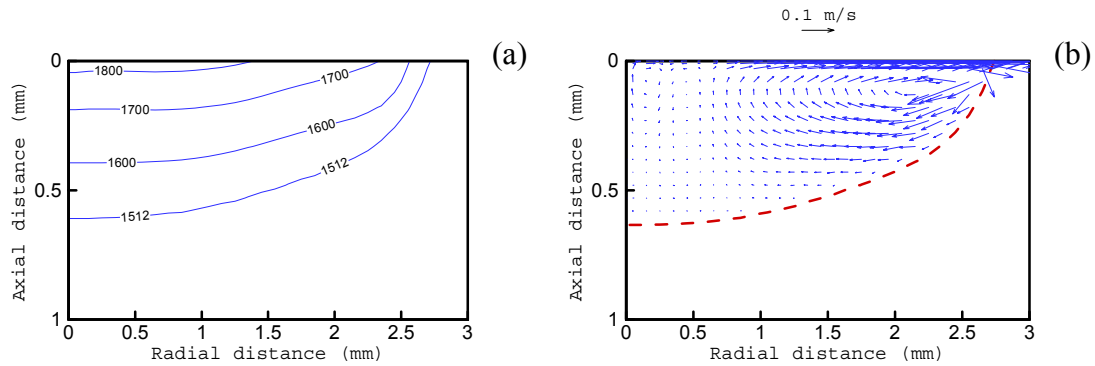
Figure 6. Computed temperature and velocity fields after 1s for $\dfrac{\partial \gamma}{\partial T} = -0.0002$: a) temperature, b) velocity.
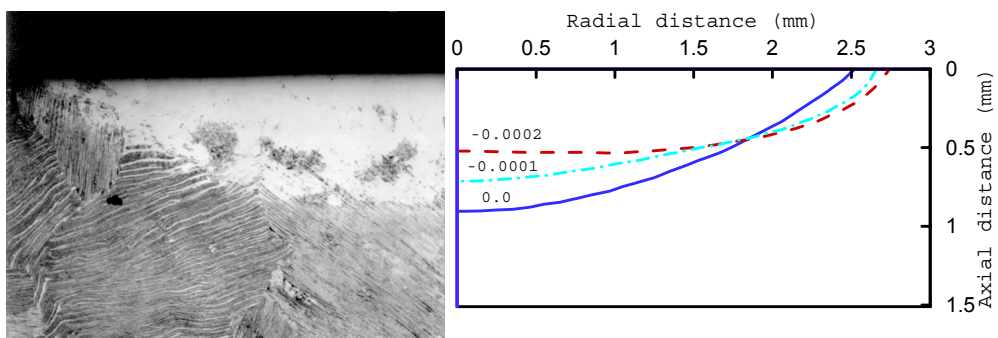
Figure 7. A comparison of the calculated and experimentally observed weld pool shape.

CONCLUSIONS

A mathematical representation has been developed for the electromagnetic force field, the transient development of the velocity field, the temperature field, and the velocity field in a metal slab for the GTA welding process. This representation relies on the statement of Maxwell's, the Navier-Stokes and the differential energy balance equations together with constitutive equations describing the current and heat input to the metal from the welding arc, in terms of the arc radius. The model has been used to investigate the effect of surface tension driven flow on the shape of γ-TiAl welds and to estimate the surface tension-temperature coefficient of molten γ-TiAl alloys through direct comparison to experimental data. The results of this study suggest that the surface tension of these alloys is almost independent of temperature. Work in progress consists of testing these findings against a broader range of experimental data.

ACKNOWLEDGEMENTS

REFERENCES

ALLEN, B.C., (1963), "The surface tension of liquid transition metals at their melting points", *Trans. AIME*, **227**, 1175-1183.

KELLY, T., (1992), "Repair welding of gamma titanium aluminide castings", *Proc. 3rd International SAMPE Metals Conference*, SAMPE, Covina, CA, 1992, 183-191.

KIM, W.-H, FAN, H.G. and NA, S.-J, (1997), "Effect of various driving forces on heat and mass transfer in arc welding", *Numer. Heat Transfer Part A*, **32**, 633-652.

KOU, S. and SUN, D.K., (1985), "Fluid flow and weld penetration in stationary arc welds", *Metall. Trans. A*, **16A**, 203-213.

LI, B., LIANG, X. EARTHMAN, J.C., and LAVERNIA, E.J., (1996), "Two dimensional modeling of momentum and thermal behavior during spray atomization of γ-TiAl", *Acta mater.,* **44**, 2409-2420.

OREPER, G.M. and SZEKELY, J., (1984), "Heat-and fluid-flow phenomena in weld pools", *J. Fluid. Mech.,* **147**, 53-79.

PELZEL, E., (1950), "The surface tension of liquid metals and alloys", *Metal Progress*, **58**, 252–261.

THOMPSON, M.E. and SZEKELY, J., (1989), "The transient behavior of weldpools with a deformed free surface", *J. Heat Mass Transfer*, **32**, 1007-1019.

TSAI, N.S. and. EAGAR, T.W., (1985), "Distribution of the heat and current fluxes in gas tungsten arcs", *Metall. Trans. B*, **16B**, 841-846.